

UC Santa Cruz

UC Santa Cruz Previously Published Works

Title

Discovery of a Novel Dual Fungal CYP51/Human 5-Lipoxygenase Inhibitor: Implications for Anti-Fungal Therapy

Permalink

<https://escholarship.org/uc/item/8jh4b9t7>

Journal

PLOS ONE, 8(6)

ISSN

1932-6203

Authors

Hoobler, Eric K

Rai, Ganesha

Warrilow, Andrew GS

et al.

Publication Date

2013

DOI

10.1371/journal.pone.0065928

Copyright Information

This work is made available under the terms of a Creative Commons Attribution License, available at <https://creativecommons.org/licenses/by/4.0/>

Peer reviewed

Discovery of a Novel Dual Fungal CYP51/Human 5-Lipoxygenase Inhibitor: Implications for Anti-Fungal Therapy

Eric K. Hoobler¹, Ganesha Rai², Andrew G. S. Warrillow³, Steven C. Perry¹, Christopher J. Smyrniotis¹, Ajit Jadhav², Anton Simeonov², Josie E. Parker³, Diane E. Kelly³, David J. Maloney^{2*}, S. L. Kelly^{3*}, Theodore R. Holman^{1*}

1 Chemistry and Biochemistry Department, University of California Santa Cruz, Santa Cruz, California, United States of America, **2** NIH Chemical Genomics Center, National Center for Advancing Translational Sciences, Bethesda, Maryland, United States of America, **3** Institute of Life Science, College of Medicine, Swansea University, Swansea, Wales, United Kingdom

Abstract

We report the discovery of a novel dual inhibitor targeting fungal sterol 14 α -demethylase (CYP51 or Erg11) and human 5-lipoxygenase (5-LOX) with improved potency against 5-LOX due to its reduction of the iron center by its phenylenediamine core. A series of potent 5-LOX inhibitors containing a phenylenediamine core, were synthesized that exhibit nanomolar potency and >30-fold selectivity against the LOX paralogs, platelet-type 12-human lipoxygenase, reticulocyte 15-human lipoxygenase type-1, and epithelial 15-human lipoxygenase type-2, and >100-fold selectivity against ovine cyclooxygenase-1 and human cyclooxygenase-2. The phenylenediamine core was then translated into the structure of ketoconazole, a highly effective anti-fungal medication for seborrheic dermatitis, to generate a novel compound, ketaminazole. Ketaminazole was found to be a potent dual inhibitor against human 5-LOX (IC₅₀ = 700 nM) and CYP51 (IC₅₀ = 43 nM) *in vitro*. It was tested in whole blood and found to down-regulate LTB₄ synthesis, displaying 45% inhibition at 10 μ M. In addition, ketaminazole selectively inhibited yeast CYP51 relative to human CYP51 by 17-fold, which is greater selectivity than that of ketoconazole and could confer a therapeutic advantage. This novel dual anti-fungal/anti-inflammatory inhibitor could potentially have therapeutic uses against fungal infections that have an anti-inflammatory component.

Citation: Hoobler EK, Rai G, Warrillow AGS, Perry SC, Smyrniotis CJ, et al. (2013) Discovery of a Novel Dual Fungal CYP51/Human 5-Lipoxygenase Inhibitor: Implications for Anti-Fungal Therapy. PLoS ONE 8(6): e65928. doi:10.1371/journal.pone.0065928

Editor: Daotai Nie, Southern Illinois University School of Medicine, United States of America

Received: November 21, 2012; **Accepted:** May 2, 2013; **Published:** June 24, 2013

Copyright: © 2013 Holman et al. This is an open-access article distributed under the terms of the Creative Commons Attribution License, which permits unrestricted use, distribution, and reproduction in any medium, provided the original author and source are credited.

Funding: This work was supported by the National Institutes of Health (GM56062 (TRH) S10-RR20939 (UCSC MS Equipment grant), the Welsh Government (SLK) and the ERDF, via the Beacon project (SLK). The funders had no role in study design, data collection and analysis, decision to publish, or preparation of the manuscript.

Competing Interests: The authors have declared that no competing interests exist.

* E-mail: maloneyd@mail.nih.gov (DJM); s.l.kelly@swansea.ac.uk (SLK); holman@ucsc.edu (TRH)

Introduction

Human 5-lipoxygenase (5-LOX) has long been considered a possible therapeutic target for inflammatory diseases. Asthma is the principle disease target, however numerous other diseases have been postulated in the literature as possible targets for 5-LOX inhibition, such as allergic rhinitis, chronic obstructive pulmonary disease, idiopathic pulmonary fibrosis, atherosclerosis, ischemia-reperfusion injury, atopic dermatitis and acne vulgaris [1–6]. The role of 5-LOX in the latter disease, acne vulgaris, has been shown to be related to the production of sebum in the derma [7]. 5-LOX has also been implicated in another skin disease, seborrheic dermatitis (i.e. dandruff) [8]. The involvement of 5-LOX in dandruff is because many systemic and superficial fungal infections are associated with inflammation. Ketoconazole is a widely used anti-fungal agent that is currently utilized as an active ingredient in anti-dandruff shampoo [9,10] and previously for a wide range of fungal infections. Its mode of action is by inhibiting fungal sterol 14 α -demethylase (Erg11 or CYP51) during ergosterol biosynthesis, thus retarding fungal growth [11]. However, it has been proposed that part of its effectiveness is due to its anti-inflammation activity,

since it also weakly inhibits 5-LOX [12]. The anti-inflammatory activity of ketoconazole has also been seen for itraconazole, a similar anti-fungal therapeutic [13], which suggests a common theme for effective dandruff agents, dual anti-fungal/anti-inflammatory targeting. Nevertheless, the potency for ketoconazole and itraconazole against 5-LOX is poor, with IC₅₀ values greater than 50 μ M for both molecules, which indicates a potential for improvement in their anti-inflammatory activity [12,13].

Numerous inhibitors for 5-LOX have been reported [14–17], which can be generally classified into three categories, reductive, iron ligands and competitive/mixed inhibitors [6,18,19] (Figure 1), however, only one compound has been approved as a drug, zileuton [20,21]. Zileuton is a potent and selective 5-LOX inhibitor but its mode of action is unusual for a therapeutic [19,22]. It contains an *N*-hydroxyurea moiety, which is proposed to chelate to the active enzyme's ferric ion and reduce it to the inactive ferrous ion [16,22,23]. In general, chelation/reduction is not considered a viable mode of inhibition for a therapeutic since metal chelation tends toward promiscuous behavior with other metalloproteins and reductive inhibitors can be chemically inactivated in the cell [16,18,19]. Nevertheless, zileuton has been

shown to not only be selective against 5-LOX but also efficacious in the cell [20–22], which presents this class of inhibitors as a viable chemotype for 5-LOX inhibition. Other chelative inhibitors, such as nordihydroguaiaretic acid (NDGA) [24–26] are also reductive due to the facile nature of inner sphere electron reduction. NDGA contains a catechol moiety, which binds to the active site ferric ion, reducing it to the ferrous ion, with the concomitant oxidation of the catechol moiety to the semiquinone. This reactivity has previously been seen with the metalloenzyme, catechol dioxygenase, whose catechol substrate is activated to the semiquinone by the active site ferric ion for oxidation by molecular oxygen [25,27,28]. There is also a sub-classification of reductive inhibitors that do not chelate the active site iron. The mechanism for these inhibitors is most likely long-range electron transfer, but no direct proof has been found for this mechanism. Recent efforts by the pharmaceutical industry have focused on non-reductive inhibitors of 5-LOX (see Figure 1; setileuton and PF-4191834), however, these appear to have been discontinued during Phase II clinical trials [29,30]. In the current publication, phenylenediamine derivatives are presented as highly selective, non-chelative, reductive inhibitors towards 5-LOX. For one derivative, the phenylenediamine core has been translated into the ketoconazole structure, generating a novel compound that demonstrates dual CYP51/5-LOX inhibitory properties. This new chemical entity, which combines anti-inflammatory and antifungal activities, is presented as a possible novel therapeutic against both the fungal and inflammatory causes of disease.

Materials and Methods

General methods for chemistry

All air or moisture sensitive reactions were performed under positive pressure of nitrogen with oven-dried glassware. Anhydrous solvents such as dichloromethane, *N,N*-dimethylformamide (DMF), acetonitrile, methanol and triethylamine were purchased from Sigma-Aldrich. Preparative purification was performed on a Waters semi-preparative HPLC system. The column used was a Phenomenex Luna C18 (5 micron, 30×75 mm) at a flow rate of 45 mL/min. The mobile phase consisted of acetonitrile and water (each containing 0.1% trifluoroacetic acid). A gradient of 10% to 50% acetonitrile over 8 minutes was used during the purification. Fraction collection was triggered by UV detection (220 nm). Analytical analysis was performed on an Agilent LC/MS (Agilent Technologies, Santa Clara, CA). Method 1: A 7 minute gradient of 4% to 100% Acetonitrile (containing 0.025% trifluoroacetic

acid) in water (containing 0.05% trifluoroacetic acid) was used with an 8 minute run time at a flow rate of 1 mL/min. A Phenomenex Luna C18 column (3 micron, 3×75 mm) was used at a temperature of 50°C. Method 2: A 3 minute gradient of 4% to 100% Acetonitrile (containing 0.025% trifluoroacetic acid) in water (containing 0.05% trifluoroacetic acid) was used with a 4.5 minute run time at a flow rate of 1 mL/min. A Phenomenex Gemini Phenyl column (3 micron, 3×100 mm) was used at a temperature of 50°C. Purity determination was performed using an Agilent Diode Array Detector for both Method 1 and Method 2. Mass determination was performed using an Agilent 6130 mass spectrometer with electrospray ionization in the positive mode. ¹H NMR spectra were recorded on Varian 400 MHz spectrometers. Chemical shifts are reported in ppm with undeuterated solvent (DMSO-*d*₆ at 2.49 ppm) as internal standard for DMSO-*d*₆ solutions. All of the analogues tested in the biological assays have purity greater than 95%, based on both analytical methods. High resolution mass spectrometry was recorded on Agilent 6210 Time-of-Flight LC/MS system. Confirmation of molecular formula was accomplished using electrospray ionization in the positive mode with the Agilent Masshunter software (version B.02).

Synthetic procedures and characterization data for compounds **1**, **2**, **6**, **8**, **12** and ketaminazole can be found in Supporting Information (File S1).

Overexpression and purification of 5-human lipoxygenase, 12-human lipoxygenase, and the 15-human lipoxygenases

Human reticulocyte 15-lipoxygenase-1 (15-LOX-1) [31] and human platelet 12-lipoxygenase (12-LOX) [31] and human prostate epithelial 15-lipoxygenase-2 (15-LOX-2) [32] were expressed as *N*-terminally, His6-tagged proteins and purified to greater than 90% purity [33]. Human leukocyte 5-lipoxygenase was expressed as a non-tagged protein and used as a crude ammonium sulfate protein fraction, as published previously [17].

Lipoxygenase UV-based inhibitor assay

Inhibitor potencies were evaluated through use of the standard UV-based inhibitor assay. The initial rates were determined by following the formation of the conjugated diene product at 234 nm ($\epsilon = 25,000 \text{ M}^{-1} \text{ cm}^{-1}$) with a Perkin-Elmer Lambda 40 UV/Vis spectrophotometer at one substrate concentration and varying inhibitor concentrations. All reactions were 2 mL in volume and constantly stirred using a magnetic stir bar at room

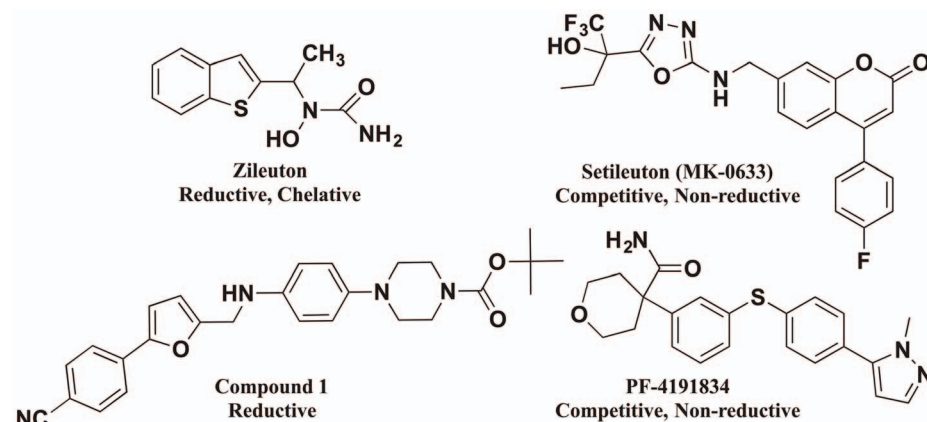


Figure 1. Structures of LOX inhibitors.
doi:10.1371/journal.pone.0065928.g001

temperature (23°C), with the enzyme specific buffer conditions outlined in Table 1. The substrate used for the various isozymes was arachidonic acid (AA) for 5-LOX, 12-LOX, and 15-LOX-2 and linoleic acid (LA) for 15-LOX-1, where concentrations were quantitatively determined by allowing the enzymatic reaction to go to completion. IC₅₀ values were obtained by determining the initial rate at various inhibitor concentrations and plotting them against inhibitor concentration, followed by a hyperbolic saturation curve fit. The data used for the saturation curves were performed in duplicate or triplicate, depending on the quality of the data. It should be noted that all of the potent inhibitors displayed greater than 80% maximal inhibition, unless otherwise stated in the tables. Inhibitors were stored at -20°C in DMSO. As a result of screening with a semi-purified protein there was concern whether the 5-LOX concentration was approaching the inhibitor concentration for our most potent inhibitors, which would affect the Henri-Michaelis-Menten approximation. In order to investigate whether the enzyme concentration was approaching the IC₅₀ value, we compared our IC₅₀ values of two high potency 5-LOX inhibitors to that in the literature. Setileuton displayed an IC₅₀ value of 60±6 nM, in good agreement with the literature value of 45±10 nM, and zileuton displayed an IC₅₀ value of 560±80 nM, in good agreement with the literature value of 500±100 nM [2,13]. The solvent isotope effect of the inhibitor IC₅₀ was investigated utilizing the same conditions and methods as stated above. The pH of the buffered D₂O was determined as reported previously [34].

Cyclooxygenase assay

Ovine COX-1 (Cat. No. 60100) and human COX-2 (Cat. No. 60122) were purchased from Cayman chemical. Approximately 2 µg of either COX-1 or COX-2 were added to buffer containing 100 µM AA, 0.1 M Tris-HCl buffer (pH 8.0), 5 mM EDTA, 2 mM phenol and 1 µM hematin at 37°C. Data was collected using a Hansatech DW1 oxygen electrode chamber, as described before [35]. Inhibitor or vehicle were mixed with the respective COX in buffer within the electrode cell, the reaction was initiated by the addition of AA, followed by monitoring of rate of oxygen consumption. Ibuprofen, aspirin and indomethacin, and the carrier solvent, DMSO, were used as positive and negative controls, respectively.

Human blood LTB₄ inhibition assay

Whole human blood was obtained from healthy volunteers from within the Student Health Center. These studies were approved by the UCSC Institutional Review Board (IRB) and informed consent was obtained from all donors before blood draw. The whole blood was dispensed in 150 µL samples followed by addition of inhibitor or control (vehicle, DMSO), and incubated for 15 min at 37°C. The mixture was then stimulated by introduction of the calcium

ionophore, A23817, (freshly diluted from a 50 mM DMSO stock to 1.5 mM in Hanks balanced salt solution), and incubated for 30 min at 37°C. Samples were then centrifuged at 1,500 rpm (300 g) for 10 min at 4°C and the supernatant diluted between 20 and 50-fold (batch dependent) for LTB₄ detection, using an ELISA detection kit (Cayman Chemicals Inc.). Inhibitors were added at 10 µM concentrations [36–38] and the IC₅₀ values were generated using a one point IC₅₀ estimation equation.

Pseudoperoxidase activity assay

The reductive properties of the inhibitors were determined by monitoring the pseudoperoxidase activity of lipoxygenase in the presence of the inhibitor and 13-(S)-hydroperoxyoctadecadienoic acid (13-HPODE). Activity is monitored by direct measurement of the product degradation following the decrease of absorbance at 234 nm using a Perkin-Elmer Lambda 40 UV/Vis spectrometer (50 mM Sodium Phosphate (pH 7.4), 0.3 mM CaCl₂, 0.1 mM EDTA, 0.01% Triton X100, 10 µM 13-HPODE). All reactions were performed in 2 mL of buffer and constantly stirred with a rotating stir bar (23°C). Reaction was initiated by addition of 10 µM inhibitor (a 1 to 1 ratio to 13-HPODE), and a positive result for activity reflected a loss of greater than 40% of product absorption at 234 nm. The control inhibitors for this assay were zileuton, a known reductive inhibitor [18], and setileuton, a competitive inhibitor [29].

Inhibitor modeling

Grid generation and flexible ligand docking were performed using Glide, while energy minimization and ligand preparation of inhibitors was done with LigPrep. LigPrep and Glide are both products of Schrodinger, Inc., and utilize energy functions to generate and rank models of ligand 3D structures and ligand-protein interactions, respectively. The crystal structure of stable human 5-lipoxygenase (PDB ID: 3O8Y) was used to generate a Glide grid in which to carry out docking algorithms with our inhibitors. This structure contains several point mutations that remove destabilizing sequences, but since none of these are located at the active site of the enzyme, it is reasonable to assume the mutant structure is an accurate model of the wild-type active site. Positional constraints at the catalytic iron and at hydrophobic pockets within the active site were prepared and utilized intermittently during different docking calculations. Poses generated from ligand docking were ranked according to their GlideScores.

CYP51 protein studies

C. albicans CYP51 (CaCYP51) and *Homo sapiens* CYP51 (HsCYP51) proteins were expressed in *E. coli* using the pCWori⁺ vector, isolated and purified as previously described [39,40] to over 90% purity. Native cytochrome P450 concentrations were

Table 1. Buffer conditions for IC₅₀ assays, with constant substrate concentration and varying inhibitor concentration^a.

Enzyme	[Enzyme]	Substrate (µM)	pH	Buffer
5-LOX	crude	10 (µM) AA	7.3	25 mM HEPES, 0.3 mM CaCl ₂ , 0.1 mM EDTA, 0.2 mM ATP, 0.01% Triton X-100
12-LOX	~40 nM	10 (µM) AA	8.0	25 mM HEPES, 0.01% Triton X-100
15-LOX-1	~20 nM	10 (µM) LA	7.5	25 mM HEPES, 0.01% Triton X-100
15-LOX-2	~100 nM	30 (µM) AA	7.5	25 mM HEPES, 0.01% Triton X-100

^aThe UV-based manual inhibition data (3 replicates) were fit as described in the Materials and Methods section.
doi:10.1371/journal.pone.0065928.t001

determined by reduced carbon monoxide difference spectra [41], based on an extinction coefficient of $91 \text{ mM}^{-1} \text{ cm}^{-1}$ [42,43]. Binding of azole antifungal agents to $5 \text{ }\mu\text{M}$ CaCYP51 and $5 \text{ }\mu\text{M}$ HsCYP51 were performed as previously described [39,44], using 0.25 and 0.5 mg mL^{-1} stock solutions of ketoconazole and ketaminazole in DMSO. Azole antifungal agents were progressively titrated against the CYP51 protein in 0.1 M Tris-HCl (pH 8.1) and 25% (wt/vol) glycerol, with the spectral difference determined after each incremental addition of azole. The dissociation constant (K_d) of the enzyme-azole complex was determined by nonlinear regression (Levenberg-Marquardt algorithm) of $\Delta A_{\text{peak-trough}}$ against azole concentration using a rearrangement of the Morrison equation [45] and fitted by the computer program ProFit 6.1.12 (QuantumSoft, Zurich, Switzerland).

IC_{50} determinations were performed using the CYP51 reconstitution assay system previously described [46,47], containing $1 \text{ }\mu\text{M}$ CaCYP51 or $0.3 \text{ }\mu\text{M}$ HsCYP51, $2 \text{ }\mu\text{M}$ human cytochrome P450 reductase, $50 \text{ }\mu\text{M}$ lanosterol, $50 \text{ }\mu\text{M}$ dilaurylphosphatidylcholine, 4.5% (wt/vol) 2-hydroxypropyl- β -cyclodextrin, 0.4 mg mL^{-1} isocitrate dehydrogenase, 25 mM trisodium isocitrate, 50 mM NaCl, 5 mM MgCl_2 and 40 mM MOPS (pH~7.2). Azole antifungal agents were added in $5 \text{ }\mu\text{L}$ DMSO followed by incubation for 5 minutes at 37°C prior to assay initiation with 4 mM β -NADPH $_{\text{NAD}}$, with shaking for a further 10 minutes at 37°C . Sterol metabolites were recovered by extraction with ethyl acetate followed by derivatization with *N,O*-bis(trimethylsilyl)trifluoroacetamide and tetramethylsilane prior to analysis by gas chromatography mass spectrometry [48]. The term IC_{50} is defined as the inhibitor concentration required for a 50% inhibition of the CYP51 reaction under the stated assay conditions.

Results and Discussion

Our laboratories have previously utilized a high-throughput screen to discover inhibitors against 12-LOX [63] and 15-LOX-1 [35]. In the process of screening the 15-LOX-1 “hits”, we serendipitously discovered a novel 5-LOX inhibitor with a phenylenediamine core moiety, compound **1**. Due to its chemical nature, the mode of inhibition was postulated to be due to reduction of the active site ferric atom. As mentioned in the introduction, reductive inhibition of lipoxygenase is a very effective mode of action, with many reductive inhibitors having sub-micromolar IC_{50} values [5,6,16,19]. This fact is indicative of both the ease with which the active site ferric can be reduced and the importance of the oxidation state of the iron. With this in mind, the phenylenediamine parent compound (**1**) was modified to change its reduction potential (Figure 2) [49]. Modifications of the phenylenediamine core, such as atom substitutions of the nitrogens with carbon or oxygen (**2** and **3**, respectively), or the insertion of two additional nitrogen atoms into the core phenyl group (**4**, **5**), resulted in complete loss of inhibition. Interestingly, substitution of only one nitrogen into the core phenyl ring (**6**) did not lower potency dramatically, nor did methylation of the nitrogen (**7**).

The pseudoperoxidase assay, was subsequently conducted with these inhibitors to establish their reductive activity against 5-LOX (Figure 2). From these data, it was demonstrated that the pseudoperoxidase activity paralleled their inhibitor potency, consistent with changes in the reductive potential of the inhibitors. Similar alterations of the core phenylenediamine structure were previously used in a similar manner to determine the relationship between potency and reductive properties [50–53]. For comparison, zileuton and setileuton were screened as positive controls,

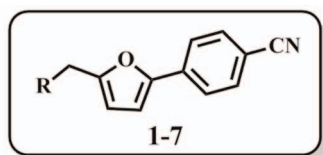
with zileuton being reductive and setileuton being non-reductive in their mechanism of inhibition.

Interpreting IC_{50} values for reductive inhibitors is challenging because their relative potency is dependent on a combination of both their reactivity with the active site iron and their binding affinity. The binding affinity was therefore investigated by changing the substituents on either side of the phenylenediamine core. As seen in Figure 3, the chemotype core tolerated a large range of modifications, such as changing the steric bulk on either side of the phenylenediamine core. Only one modification in this small set of compounds showed a greater than 10-fold decrease in potency, **10**, which was surprising given the activity of related oxazoles **8** and **9**. The lack of dependence between inhibitor potency and inhibitor structure suggests that the active site can accommodate a variety of inhibitor shapes and sizes. These findings are consistent with the large size of the 5-LOX active site [54] and the re-occurrence of large 5-LOX inhibitors discovered [6,16,19].

Selectivity of the inhibitor chemotype was evaluated by screening a variety of LOX isozymes with a small subset of compounds (Table 2). Strong selectivity was displayed against 5-LOX relative to the other isozymes, with selectivity ratios ranging from 80-fold for 12-LOX, 75-fold for 15-LOX-1, and 30-fold for 15-LOX-2, for the least selective analogues (Table 2). The chemotype also displayed strong selectivity when assayed against cyclooxygenase (COX), with a 140-fold selectivity versus COX-1, and a 240-fold selectivity versus COX-2. These combined results indicate this chemotype has a strong preference/selectivity against 5-LOX versus other AA processing enzymes. As controls, zileuton and setileuton were utilized as selective inhibitors of 5-LOX [20,21,29].

A few inhibitors were then tested for efficacy in whole human blood, which is known to express 5-LOX upon activation by an ionophore. **1** and **13** displayed roughly 50% inhibition at $10 \text{ }\mu\text{M}$ drug dosing in the whole blood, while the positive control, setileuton, was found to inhibit 100% at $10 \text{ }\mu\text{M}$ (Table 3). Compound **15** was also tested, but the potency was shown to be weak, with less than 10% inhibition at $10 \text{ }\mu\text{M}$ (Table 3). The cellular enzyme inhibition for **1**, **13** and setileuton are diminished relative to the isolated-enzyme inhibitor values (Figure 2). This result, along with other analogues failing to display high potency, could indicate poor permeability, plasma protein binding, non-specific interactions or metabolism of the inhibitors by the cell.

The determination that the reductive phenylenediamine core was the key potency component and that the addition of large functionalities to either side of the phenylenediamine core was well tolerated led us to consider the similarity between the phenylenediamine chemotype and ketoconazole (Figure 4). Ketoconazole is a CYP51 inhibitor with an azole moiety that targets the active site heme and is a potent antifungal medication [8,9]. In addition, ketoconazole was previously determined to inhibit 5-LOX and have anti-inflammatory properties, although weakly [12]. Considering the similarity of ketoconazole to our chemotype, we hypothesized that by adding the phenylenediamine core to ketoconazole, we could improve its 5-LOX potency by making it a reductive inhibitor and thus increasing its anti-inflammatory properties. We subsequently modified the structure of ketoconazole to include a phenylenediamine core to generate a novel compound, ketaminazole (**16**) and found that its potency against 5-LOX increased over 70-fold compared to ketoconazole (Figure 4) and that it was a reductive inhibitor, as seen by its activity in the pseudoperoxidase assay (Figure 4). The selectivity of the ketaminazole (**16**) was also investigated and found to preferentially inhibit 5-LOX over 100 times better than that of 12-LOX, 15-



Compound	R	Reductive Activity	IC ₅₀ (μM) [± SD (μM)]
Zilueton	NA	Yes	0.56 [0.08]
Setileuton	NA	No	0.06 [0.007]
1		Yes	0.17 [0.05]
2		No	>150
3		No	>150
4		No	>150
5		No	>150
6		Yes	1.1 [0.2]
7		Yes	2.7 [0.4]

Figure 2. Representative analogues evaluated for pseudoperoxidase activity and IC₅₀ potency (μM), with errors in brackets. The UV-based manual inhibition data (3 replicates) were fit as described in the Materials and Methods section. doi:10.1371/journal.pone.0065928.g002

LOX-1, 15-LOX-2, COX-1 and COX-2 (Figure 4). This is most likely due to the large active site of 5-LOX compared to the other human LOX isozymes. Ketaminazole (**16**) was also tested in whole human blood and shown to display cellular activity. Like the smaller phenylenediamine inhibitors (**1**, **13** and **15**), ketaminazole's cellular potency is lower relative to its *in vitro* potency, displaying an approximately 20-fold reduction (Table 3). The magnitude of the potency in whole blood is not consistent between all the phenylenediamine inhibitors tested. This indicates that the structural differences between the phenylenediamine inhibitors have an effect on their cellular potency, supporting the hypothesis that cellular factors, other than the phenylenediamine core, are important. Gratifyingly, ketaminazole (**16**) displayed a better potency against 5-LOX in whole blood relative to ketoconazole, however, the magnitude of this difference was not as great as their *in vitro* difference. This is surprising since their only structural difference is the substitution of an amine for the ether linkage. It could be that the polarity change of the inhibitors changes their cellular uptake or that the reductive state of the ketaminazole is being compromised in the cell. Further cellular studies are required to probe these hypotheses further.

In addition to kinetic data, the importance of the phenylenediamine core for reductive inhibition was further supported using computational methods. Molecular modeling of possible inhibitor binding modes within the active site was initiated by deprotonation of the amine groups at the phenylenediamine core and energy

minimization of the compounds with LigPrep [55,56]. The inhibitors listed in of the Figures/Tables above were then docked against the crystal structure of modified protein, Stable-5-LOX (3O8Y), using Glide's "XP" (extra-precision) mode [55,56]. Different trials, with varying Van der Waals scaling factors and alternating positional or hydrophobic constraints linking the inhibitor to the active site, resulted in the occurrence of high-ranking binding poses depicting the deprotonated amine nitrogen within 10 angstroms of the catalytic iron for several inhibitors. The docking results of these inhibitors support the hypothesis that the reduction of the ferric iron could be caused by the phenylenediamine core, either through an inner sphere (direct coordination to the iron) or outer sphere (through space) mechanism [57]. Docking of the larger inhibitors, ketoconazole (Figure 5a) and ketaminazole (**16**) (Figure 5b), generated poses with similar Glide docking scores to the other inhibitors studied, suggesting a comparable binding mode despite the differences in IC₅₀ values. In several high-ranking binding poses, the amine/ester core of ketaminazole (**16**) was observed to be within 5 angstroms of the catalytic iron (Figure 5b), supportive of the hypothesis that the phenylenediamine core reduces the active site iron.

The docking poses of the phenylenediamine inhibitors suggest that their amine moieties could be possible conduits of iron reduction, through space via an outer sphere mechanism [57]. However, the docking poses also suggest the active site iron-hydroxide moiety could possibly abstract a hydrogen atom from

Compound	R	5-LOX IC ₅₀ (μM) [± SD (μM)]
1		0.17 [0.05]
8		0.10 [0.06]
9		1.5 [0.2]
10		>150
11		1.1 [0.10]
12		2.6 [0.3]
13		0.52 [0.07]
14		0.33 [0.07]
15		0.6 [0.1]

Figure 3. 5-LOX IC₅₀ values of representative analogues (μM), with errors in brackets. The UV-based manual inhibition data (3 replicates) were fit as described in the Materials and Methods section.
doi:10.1371/journal.pone.0065928.g003

the amine by an inner sphere mechanism, as is seen in the natural mechanism of LOX with its fatty acid substrate [58]. To test this hypothesis, **13** was incubated in D₂O buffer, to deuterate the phenylenediamine core amine, and its IC₅₀ value compared to the protonated amine in H₂O. A 2.4-fold increase in the IC₅₀ for **13** was observed in D₂O, which is well below the kinetic isotope effect expected for hydrogen atom abstraction [57], suggestive of a

proton independent outer sphere reductive mechanism. To further verify this proton-independent reductive mechanism, **1** and **7** (containing the protonated and methylated amine, respectively) were also investigated and both were shown to have similar increases in IC₅₀ values in D₂O relative to H₂O, suggesting the effect does not involve the amine proton.

Table 2. Selectivity profile of representative analogues (μM), with errors in parentheses^a.

Compound	5-LOX	12-LOX	15-LOX-1	15-LOX-2	COX-1	COX-2
1	0.17 (0.05)	>150	>150	>150	>50	>150
13	0.52 (0.07)	>50	>50	>50	>150	>150
14	0.33 (0.07)	>150	>25	10	>150	N/D ^b
15	0.60 (0.1)	>50	>150	>50	N/D	N/D
Setileuton	0.060 (0.007)	>150	>150	>150	>150	>50
Zileuton	0.56 (0.08)	>150	>50	>150	>150	N/D

^aThe UV-based manual inhibition data (3 replicates) were fit as described in the Materials and Methods section.

^bN/D=Not determined.

doi:10.1371/journal.pone.0065928.t002

Table 3. Whole human blood activity profile of representative analogues^a.

Compound	Inhibition (%)
Setileuton	100 (11)
Cicloproxin	34 (2)
Ketaminazole (16)	45 (10)
Ketoconazole	25 (3)
1	65 (14)
13	54 (11)
15	8 (1)

^aThe ELISA absorption-based inhibition data (3 replicates) were fit as described in the Materials and Methods section. Compounds were assayed at 10 μ M. doi:10.1371/journal.pone.0065928.t003

In order to evaluate the concept of an improved anti-inflammatory effect combined with antifungal potency, we examined the selectivity of ketoconazole and ketaminazole (**16**) against the human and *C. albicans* CYP51 proteins, HsCYP51 and CaCYP51 respectively. Binding ketoconazole and ketaminazole (**16**) with both CaCYP51 and HsCYP51 produced strong type II difference spectra (Figure 6) signifying direct coordination as the sixth ligand of the heme prosthetic group of CYP51 [58,59]. Ketoconazole and ketaminazole (**16**) both bound tightly to CaCYP51 with K_d values of 27 ± 5 and 43 ± 5 nM, respectively. Tight binding is observed when the K_d for the ligand is similar to or less than the concentration of CYP51 present [60]. The similar K_d values obtained for ketoconazole and ketaminazole (**16**) suggest both azoles would be equally effective as antifungal agents against wild-type CaCYP51. This is understandable since the CYP51 potency of this class of molecules is predominantly due to their azole moiety, which is quite distant from the phenylenediamine core of ketaminazole (**16**). This data also compares with K_d values of 10 to 50 nM previously obtained for clotrimazole, econazole, fluconazole, itraconazole, ketoconazole, miconazole and voriconazole with CaCYP51 [39]. Ketoconazole bound 17-fold more tightly to HsCYP51 ($K_d = 42 \pm 16$ nM) compared to ketaminazole (**16**) ($K_d = 731 \pm 69$ nM), in contrast to the 1.6-fold difference observed with CaCYP51, suggesting that ketaminazole would interfere less with the host HsCYP51 and possibly other human CYPs than ketoconazole, conferring a therapeutic advantage. These results compare well with the previously reported K_d values of <100 nM for clotrimazole, econazole and miconazole,

~ 180 nM for ketoconazole and ~ 70 μ M for fluconazole with HsCYP51 [40].

The IC₅₀ CYP51 reconstitution assay results (Figure 7) mirrored those of the azole binding results. CaCYP51 was strongly inhibited by both ketoconazole and ketaminazole (**16**) with IC₅₀ values of ~ 0.5 and ~ 0.9 μ M, respectively, confirming that both azoles bound tightly to CaCYP51. Interestingly, at 4 μ M ketaminazole (**16**), CaCYP51 retained $\sim 15\%$ CYP51 activity suggesting that lanosterol can displace ketaminazole (**16**) from CaCYP51 leading to ketaminazole (**16**) being a less effective inhibitor of fungal CYP51 enzymes *in vitro* than ketoconazole. HsCYP51 was less severely inhibited by both ketoconazole and ketaminazole (**16**) with IC₅₀ values of ~ 5 and ~ 16 μ M, respectively. This indicates that azole binding was less tight and suggested lanosterol can displace ketoconazole and especially ketaminazole (**16**) from HsCYP51. At 95 μ M ketoconazole HsCYP51 was inactivated in contrast to the $\sim 30\%$ CYP51 activity remaining in the presence of 155 μ M ketaminazole (**16**). The 3-fold higher IC₅₀ value of ketaminazole (**16**) over ketoconazole with HsCYP51 confirmed that ketaminazole (**16**) would be less disruptive to the CYP51 function of the host homolog than ketoconazole, conferring a therapeutic advantage for use as an antifungal agent. It should be noted that both itraconazole and posaconazole, both effective antifungal agents, could also have a phenylenediamine incorporated into their structures, thus conferring dual anti-fungal/anti-inflammatory properties on these therapeutics as well. We are currently investigating the properties of these modified anti-fungal agents further, with the hope of utilizing the phenylenediamine moiety as a simple modification for adding 5-LOX inhibitory potency to known therapeutics.

The fact that ketoconazole is both an anti-fungal and anti-inflammatory molecule is not a new phenomenon in the field of anti-fungal therapeutics. Previously, we determined that the common anti-fungal agent, chloroxine, was also a non-specific LOX inhibitor [61]. This fact suggested that the inherent selection process for the search for anti-seborrheic dermatitis agents could be responsible for the dual nature of the anti-fungal/anti-inflammatory therapeutics, such as chloroxine and ketoconazole. With this hypothesis in mind, the anti-fungal agent, ciclopirox (trade name Loprox), presented a structure that could be interpreted as a LOX inhibitor, with the *N*-hydroxyamide being a possible chelator. This was confirmed and ciclopirox was found to be both a potent inhibitor of 5-LOX (IC₅₀ = 11 ± 1 μ M) and selective versus other AA processing enzymes (Figure 4). This dual nature of many anti-seborrheic dermatitis agents suggests that

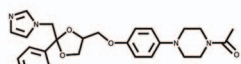
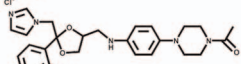
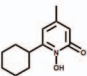
Compound	Structure	Reductive activity	5-LOX	12-LOX	15-LOX-1	15-LOX-2	COX-1	COX-2
ketoconazole		No	>50	>150	>50	>150	>50	>150
ketaminazole (16)		Yes	0.7 (0.01)	>150	>150	>150	>150	>150
ciclopirox		N/D ^b	11 (1)	>100	>100	N/D	>50	>150

Figure 4. IC₅₀ values of dual anti-fungal, anti-inflammatory inhibitors (μ M), with error in parentheses. The UV-based manual inhibition data (3 replicates) were fit as described in the Materials and Methods section. N/D=Not determined. doi:10.1371/journal.pone.0065928.g004

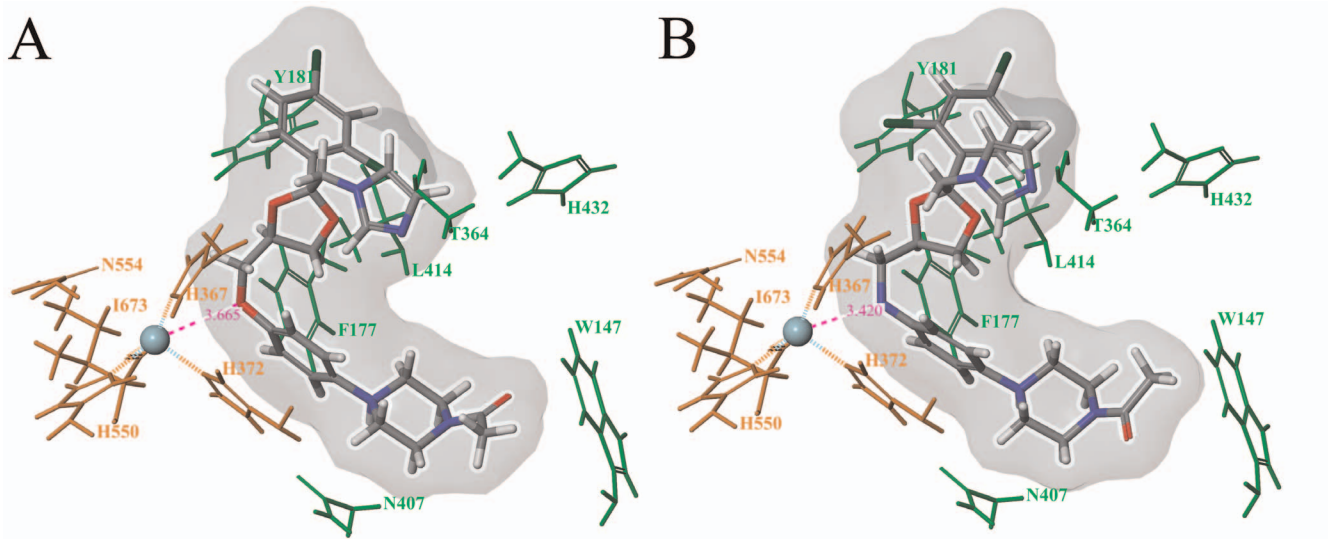


Figure 5. Docking ketoconazole (A) and ketaminazole (B) to the crystal structure of the Stable-5-LOX (PDB ID: 3O8Y). Glide docking scores and poses were similar to other high-ranking docked inhibitors. doi:10.1371/journal.pone.0065928.g005

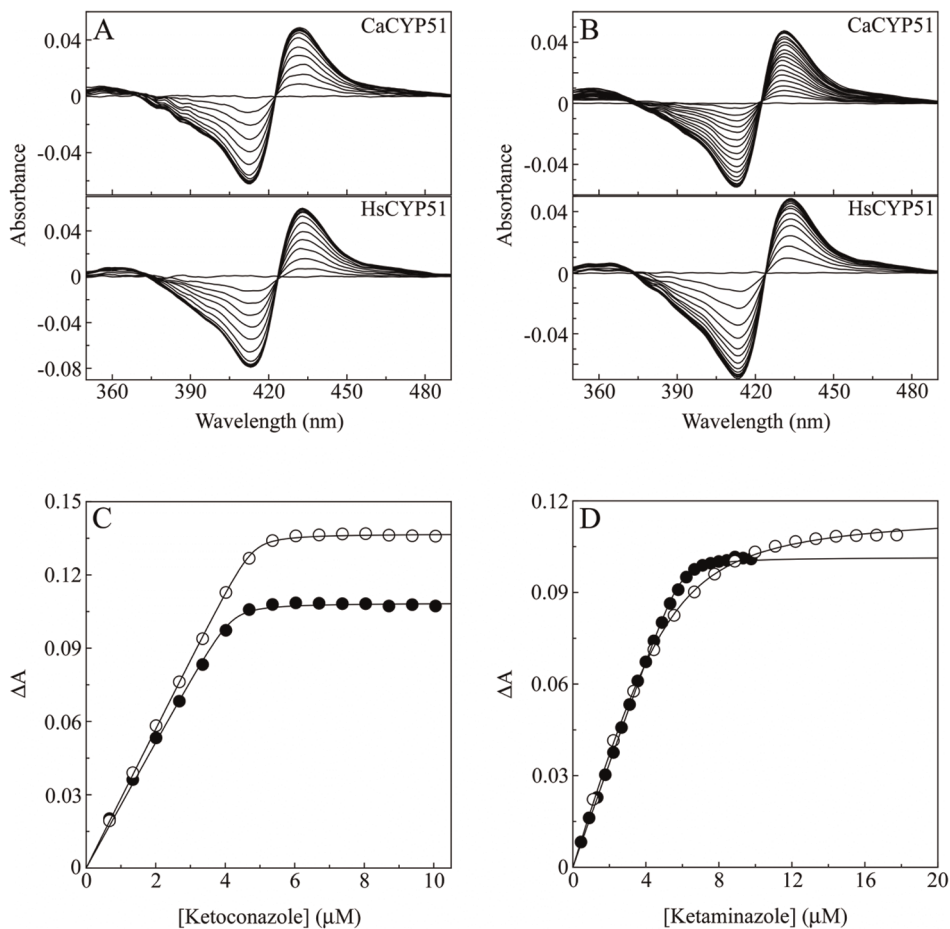


Figure 6. Binding properties of ketoconazole and ketaminazole with CaCYP51 and HsCYP51. Azole antifungals were progressively titrated against 5 μM CaCYP51 (filled circles) and 5 μM HsCYP51 (hollow circles). The resultant type II difference spectra are shown for ketoconazole (A) and ketaminazole (B). Saturation curves for ketoconazole (C) and ketaminazole (D) were constructed and a rearrangement of the Morrison equation (45) was used to fit the data. The data shown represent one replicate of the three performed. doi:10.1371/journal.pone.0065928.g006

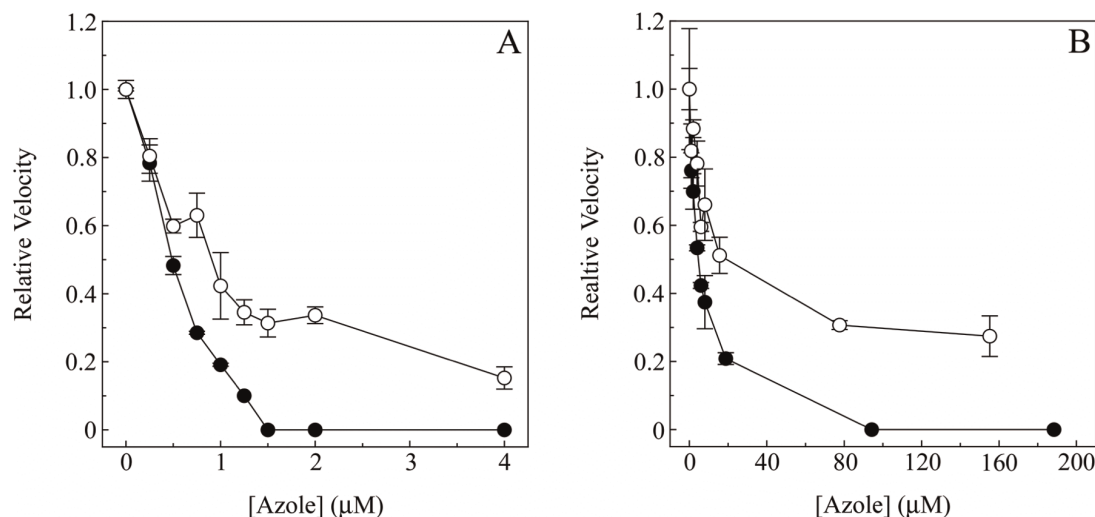


Figure 7. Determination of IC_{50} values for ketoconazole and ketaminazole with CaCYP51 and HsCYP51. CYP51 reconstitution assays (0.5-ml total volume) containing 1 μ M CaCYP51 (A) or 0.3 μ M HsCYP51 (B) were performed as detailed in Materials and Methods. Ketoconazole (solid circles) and ketaminazole (hollow circles) concentrations were varied from 0 to 4 μ M for CaCYP51 and up to 190 μ M for HsCYP51 with the DMSO concentration kept constant at 1% (vol/vol). Mean values from two replicates are shown along with associated standard deviation bars. Relative velocities of 1.0 were equivalent to 1.04 and 2.69 nmoles 14 α -demethylated lanosterol produced per minute per nmole CYP51 (min^{-1}) for CaCYP51 and HsCYP51, respectively.
doi:10.1371/journal.pone.0065928.g007

improving the 5-LOX potency of these therapeutics may be beneficial in their clinical efficacy.

Conclusion

The current data indicate that the phenylenediamine chemotype reported herein is a potent inhibitor against 5-LOX, demonstrating enzyme selectivity and cellular activity. The mechanism of action is consistent with reduction of the active site ferric ion, similar to that seen for zileuton, the only FDA approved LOX inhibitor. It is interesting to note that unlike zileuton, which chelates the iron through the *N*-hydroxyurea, the phenylenediamine chemotype lacks an obvious chelating moiety, thus differentiating it from zileuton. Structural modification around the phenylenediamine core was well tolerated, however, even relatively minor changes to the phenylenediamine moiety resulted in a loss of activity, presumably due to changes in its reduction potential. This attribute was utilized to modify the structure of ketoconazole to include the phenylenediamine moiety and produce a novel inhibitor, ketaminazole (**16**). This novel compound demonstrated an *in vitro* 40-fold increase in potency against 5-LOX relative to ketoconazole. However, in whole blood ketaminazole demonstrated only a 2-fold greater potency than ketoconazole. In addition, the overall potency of ketaminazole was

reduced by approximately 10-fold relative to its *in vitro* potency. It is currently unclear how the cellular environment is lowering the potency of ketaminazole, but pharmacokinetic investigations are currently underway to probe this further. Ketaminazole (**16**) had comparable potency against fungal CYP51 and improved selectivity against the human CYP51, relative to ketoconazole, which suggests a possible therapeutic advantage. This novel dual nature of ketaminazole (**16**), possessing both anti-fungal and anti-inflammatory activity, could potentially have therapeutic uses against fungal infections that have an anti-inflammatory component.

Supporting Information

File S1. Supporting Information on Inhibitor Synthesis and Characterization. (DOCX)

Author Contributions

Conceived and designed the experiments: EH GR AW SP CS AJ AS JP DK DM SK TH. Performed the experiments: EH GR AW SP CS AJ AS JP DK DM. Analyzed the data: EH GR AW SP CS AJ AS JP DK DM. Contributed reagents/materials/analysis tools: EH GR AW SP CS AJ AS JP DK DM. Wrote the paper: EH GR AJ AS DK DM SK TH.

References

- Rubin P, Mollison KW (2007) Pharmacotherapy of diseases mediated by 5-lipoxygenase pathway eicosanoids. Prostaglandins Other Lipid Mediat 83: 188–197.
- O'Byrne PM, Israel E, Drazen JM (1997) Antileukotrienes in the Treatment of Asthma. Annals of Internal Medicine 127: 472–480.
- Rådmark OP (2000) The Molecular Biology and Regulation of 5-Lipoxygenase. American Journal of Respiratory and Critical Care Medicine 161: S11–S15.
- Ford-Hutchinson AW, Gresser M, Young RN (1994) 5-Lipoxygenase. Annu Rev Biochem 63: 383–417.
- Wertz O, Steinhilber D (2006) Therapeutic options for 5-lipoxygenase inhibitors. Pharmacology & Therapeutics 112: 701–718.
- Pergola C, Wertz O (2010) 5-Lipoxygenase inhibitors: a review of recent developments and patents. Expert Opinion on Therapeutic Patents 20: 355–375.
- Zouboulis Ch C, Saborowski A, Boschnakow A (2005) Zileuton, an oral 5-lipoxygenase inhibitor, directly reduces sebum production. Dermatology 210: 36–38.
- Faergemann J (2000) Management of seborrheic dermatitis and pityriasis versicolor. Am J Clin Dermatol 1: 75–80.
- Faergemann J, Borgers M, Degreef H (2007) A new ketoconazole topical gel formulation in seborrheic dermatitis: an updated review of the mechanism. Expert Opinion on Pharmacotherapy 8: 1365–1371.
- Borgers M, Degreef H (2007) The role of ketoconazole in seborrheic dermatitis. Cutis 80: 359–363.
- Scheinfeld N (2008) Ketoconazole: a review of a workhorse antifungal molecule with a focus on new foam and gel formulations. Drugs Today (Barc) 44: 369–380.

12. Bectens JR, Loots W, Somers Y, Coene MC, de Clerck F (1986) Ketoconazole inhibits the biosynthesis of leukotrienes in vitro and in vivo. *Biochemical Pharmacology* 35: 883–891.
13. Steel HC, Tintinger GR, Theron AJ, Anderson R (2007) Itraconazole-mediated inhibition of calcium entry into platelet-activating factor-stimulated human neutrophils is due to interference with production of leukotriene B₄. *Clin Exp Immunol* 150: 144–150.
14. Koerberle A, Zettl H, Greiner C, Wurglics M, Schubert-Zsilavecz M, et al. (2008) Pirinixic Acid Derivatives as Novel Dual Inhibitors of Microsomal Prostaglandin E₂ Synthase-1 and 5-Lipoxygenase. *Journal of Medicinal Chemistry* 51: 8068–8076.
15. McMillan RM, Walker ER (1992) Designing therapeutically effective 5-lipoxygenase inhibitors. *Trends Pharmacol Sci* 13: 323–330.
16. Musser JH, Kreft AF (1992) 5-lipoxygenase: properties, pharmacology, and the quinolonyl(bridged)aryl class of inhibitors. *J of Med Chem* 35: 2501–2524.
17. Robinson SJ, Hoobler EK, Riener M, Loveridge ST, Tenney K, et al. (2009) Using enzyme assays to evaluate the structure and bioactivity of sponge-derived meroterpenes. *Journal of Natural Products* 72: 1857–1863.
18. Falgucyret JP, Hutchinson JH, Riendeau D (1993) Criteria for the identification of non-redox inhibitors of 5-lipoxygenase. *Biochemical Pharmacology* 45: 978–981.
19. Robert NY (1999) Inhibitors of 5-lipoxygenase: a therapeutic potential yet to be fully realized? *European Journal of Medicinal Chemistry* 34: 671–685.
20. Carter GW, Young PR, Albert DH, Bouska J, Dyer R, et al. (1991) 5-lipoxygenase inhibitory activity of zileuton. *J Pharmacol Exp Ther* 256: 929–937.
21. McGill KA, Busse WW (1996) Zileuton. *The Lancet* 348: 519–524.
22. Bell RL, Young PR, Albert D, Lanni C, Summers JB, et al. (1992) The discovery and development of zileuton: an orally active 5-lipoxygenase inhibitor. *Int J Immunopharmacol* 14: 505–510.
23. Stewart AO, Bhatia PA, Martin JG, Summers JB, Rodrigues KE, et al. (1997) Structure-activity relationships of N-hydroxyurea 5-lipoxygenase inhibitors. *J Med Chem* 40: 1955–1968.
24. Walenga RW, Showell HJ, Feinstein MB, Becker EL (1980) Parallel inhibition of neutrophil arachidonic acid metabolism and lysosomal enzyme secretion by nordihydroguaiaretic acid. *Life Sciences* 27: 1047–1053.
25. Kemal C, Louis-Flamberg P, Krupinski-Olsen R, Shorter A (1987) Reductive Inactivation of Soybean Lipoxygenase-1 by Catechols. *Biochemistry* 26: 7064–7072.
26. Whitman S, Gezginci M, Timmermann BN, Holman TR (2002) Structure-activity relationship studies of nordihydroguaiaretic acid inhibitors toward soybean, 12-human, and 15-human lipoxygenase. *J Med Chem* 45: 2659–2661.
27. Pham C, Jankun J, Skrzypczak-Jankun E, Flowers RA, Funk MO (1998) Structural and thermochemical characterization of lipoxygenase-catechol complexes. *Biochemistry* 37: 17952–17957.
28. Nelson MJ, Cowling RA, Seitz SP (1994) Structural Characterization of Alkyl and Peroxyl Radicals in Solutions of Purple Lipoxygenase. *Biochemistry* 33: 4966–4973.
29. Ducharme Y, Blouin M, Brideau C, Châteauneuf A, Gareau Y, et al. (2010) The Discovery of Setileuton, a Potent and Selective 5-Lipoxygenase Inhibitor. *ACS Medicinal Chemistry Letters* 1: 170–174.
30. Masferrer JL, Zweifel BS, Hardy M, Anderson GD, Dufield D, et al. Pharmacology of PF-4191834, a novel, selective non-redox 5-lipoxygenase inhibitor effective in inflammation and pain. *J Pharmacol Exp Ther* 334: 294–301.
31. Amagata T, Whitman S, Johnson TA, Stessman CC, Loo CP, et al. (2003) Exploring sponge-derived terpenoids for their potency and selectivity against 12-human, 15-human, and 15-soybean lipoxygenases. *J Nat Prod* 66: 230–235.
32. Deschamps JD, Gautschi JT, Whitman S, Johnson TA, Gassner NC, et al. (2007) Discovery of platelet-type 12-human lipoxygenase selective inhibitors by high-throughput screening of structurally diverse libraries. *Bioorganic & Medicinal Chemistry* 15: 6900–6908.
33. Vasquez-Martinez Y, Ohri RV, Kenyon V, Holman TR, Sepulveda-Boza S (2007) Structure-activity relationship studies of flavonoids as potent inhibitors of human platelet 12-hLO, reticulocyte 15-hLO-1, and prostate epithelial 15-hLO-2. *Bioorganic & Medicinal Chemistry* 15: 7408–7425.
34. Segraves EN, Holman TR (2003) Kinetic investigations of the rate-limiting step in human 12- and 15-lipoxygenase. *Biochemistry* 42: 5236–5243.
35. Rai G, Kenyon V, Jadhav A, Schultz L, Armstrong M, et al. (2010) Discovery of potent and selective inhibitors of human reticulocyte 15-lipoxygenase-1. *J Med Chem* 53: 7392–7404.
36. Hutchinson JH, Li Y, Arruda JM, Baccei C, Bain G, et al. (2009) 5-Lipoxygenase-Activating Protein Inhibitors: Development of 3-[3-tert-Butylsulfanyl-1-[4-(6-methoxy-pyridin-3-yl)-benzyl]-5-(pyridin-2-ylmethoxy)-1H-indol-2-yl]-2,2-dimethyl-propionic Acid (AM103). *Journal of Medicinal Chemistry* 52: 5803–5815.
37. Fogh J, Poulsen LK, Bisgaard H (1992) A specific assay for leukotriene B₄ in human whole blood. *Journal of Pharmacological and Toxicological Methods* 28: 185–190.
38. Spaethe SM, Snyder DW, Pechous PA, Clarke T, VanAlstyne EL (1992) Guinea pig whole blood 5-lipoxygenase assay: utility in the assessment of potential 5-lipoxygenase inhibitors. *Biochemical Pharmacology* 43: 377–382.
39. Warrilow AG, Martel CM, Parker JE, Melo N, Lamb DC, et al. (2010) Azole binding properties of *Candida albicans* sterol 14- α -demethylase (CaCYP51). *Antimicrob Agents Chemother* 54: 4235–4245.
40. Strushkevich N, Usanov SA, Park HW (2010) Structural basis of human CYP51 inhibition by antifungal azoles. *J Mol Biol* 397: 1067–1078.
41. Estabrook RW, Peterson JA, Baron J, Hildebrandt AG (1972) The spectrophotometric measurement of turbid suspensions of cytochromes associated with drug metabolism. *Methods Pharmacol* 2: 303–350.
42. Omura T, Sato R (1964) The Carbon Monoxide-Binding Pigment of Liver Microsomes. II. Solubilization, Purification, and Properties. *J Biol Chem* 239: 2379–2385.
43. Omura T, Sato R (1964) The Carbon Monoxide-Binding Pigment of Liver Microsomes. I. Evidence for Its Hemoprotein Nature. *J Biol Chem* 239: 2370–2378.
44. Lamb DC, Kelly DE, Waterman MR, Stromstedt M, Rozman D, et al. (1999) Characteristics of the heterologously expressed human lanosterol 14 α -demethylase (other names: P45014DM, CYP51, P45051) and inhibition of the purified human and *Candida albicans* CYP51 with azole antifungal agents. *Yeast* 15: 755–763.
45. Lutz JD, Dixit V, Yeung CK, Dickmann IJ, Zelter A, et al. (2009) Expression and functional characterization of cytochrome P450 26A1, a retinoic acid hydroxylase. *Biochem Pharmacol* 77: 258–268.
46. Lepesheva GI, Ott RD, Hargrove TY, Kleshchenko YY, Schuster I, et al. (2007) Sterol 14 α -demethylase as a potential target for antirypanosomal therapy: enzyme inhibition and parasite cell growth. *Chem Biol* 14: 1283–1293.
47. Lepesheva GI, Zaitseva NG, Nes WD, Zhou W, Arase M, et al. (2006) CYP51 from *Trypanosoma cruzi*: a phyla-specific residue in the B' helix defines substrate preferences of sterol 14 α -demethylase. *J Biol Chem* 281: 3577–3585.
48. Venkateswarlu K, Denning DW, Manning NJ, Kelly SL (1995) Resistance to fluconazole in *Candida albicans* from AIDS patients correlated with reduced intracellular accumulation of drug. *FEMS Microbiol Lett* 131: 337–341.
49. Lo HY, Man CC, Fleck RW, Farrow NA, Ingraham RH, et al. (2010) Substituted pyrazoles as novel sEH antagonist: investigation of key binding interactions within the catalytic domain. *Bioorg Med Chem Lett* 20: 6379–6383.
50. Itoh T, Nagata K, Miyazaki M, Ishikawa H, Kurihara A, et al. (2004) A selective reductive amination of aldehydes by the use of Hantzsch dihydropyridines as reductant. *Tetrahedron* 60: 6649–6655.
51. Ito S, Kubo T, Morita N, Ikoma T, Tero-Kubota S, et al. (2005) Azulene-Substituted Aromatic Amines. Synthesis and Amphoteric Redox Behavior of N,N-Di(6-azuleny)-p-toluidine and N,N,N',N'-Tetra(6-azuleny)-p-phenylenediamine and Their Derivatives. *The Journal of Organic Chemistry* 70: 2285–2293.
52. Vouros P, Biemann K (1969) The structural significance of doubly charged ion spectra. Phenylenediamine derivatives. *Organic Mass Spectrometry* 2: 375–386.
53. Sakurai H, Ritonga MTS, Shibatani H, Hirao T (2005) Synthesis and Characterization of p-Phenylenediamine Derivatives Bearing an Electron-Acceptor Unit. *The Journal of Organic Chemistry* 70: 2754–2762.
54. Gilbert NC, Bartlett SG, Waight MT, Neau DB, Boeglin WE, et al. (2011) The structure of human 5-lipoxygenase. *Science* 331: 217–219.
55. Friesner RA, Banks JL, Murphy RB, Halgren TA, Klicic JJ, et al. (2004) Glide: a new approach for rapid, accurate docking and scoring. 1. Method and assessment of docking accuracy. *J Med Chem* 47: 1739–1749.
56. Halgren TA, Murphy RB, Friesner RA, Beard HS, Frye LL, et al. (2004) Glide: a new approach for rapid, accurate docking and scoring. 2. Enrichment factors in database screening. *J Med Chem* 47: 1750–1759.
57. Lewis ER, Johansen E, Holman TR (1999) Large competitive kinetic isotope effects in human 15-LO catalysis measured by a novel HPLC method. *J Am Chem Soc* 121: 1395–1396.
58. Jefcoate CR (1978) Measurement of substrate and inhibitor binding to microsomal cytochrome P-450 by optical-difference spectroscopy. *Methods Enzymol* 52: 258–279.
59. Jefcoate CR, Gaylor JL, Calabrese RL (1969) Ligand interactions with cytochrome P-450. I. Binding of primary amines. *Biochemistry* 8: 3455–3463.
60. Copeland RA (2005) Evaluation of enzyme inhibitors in drug discovery. A guide for medicinal chemists and pharmacologists. *Methods Biochem Anal* 46: 1–265.
61. Kenyon V, Rai G, Jadhav A, Schultz L, Armstrong M, et al. (2011) Discovery of potent and selective inhibitors of human platelet-type 12-lipoxygenase. *J Med Chem* 54: 5485–5497.